

Lawrence Berkeley National Laboratory

Recent Work

Title

TRANSPORT PROPERTIES OF EXCITED NUCLEAR MATTER AND THE SHOCK-WAVE PROFILE

Permalink

<https://escholarship.org/uc/item/9704t6nn>

Author

Danielewicz, P.

Publication Date

1984-05-01



Lawrence Berkeley Laboratory

UNIVERSITY OF CALIFORNIA

RECEIVED
LAWRENCE
BERKELEY LABORATORY

JUL 5 1984

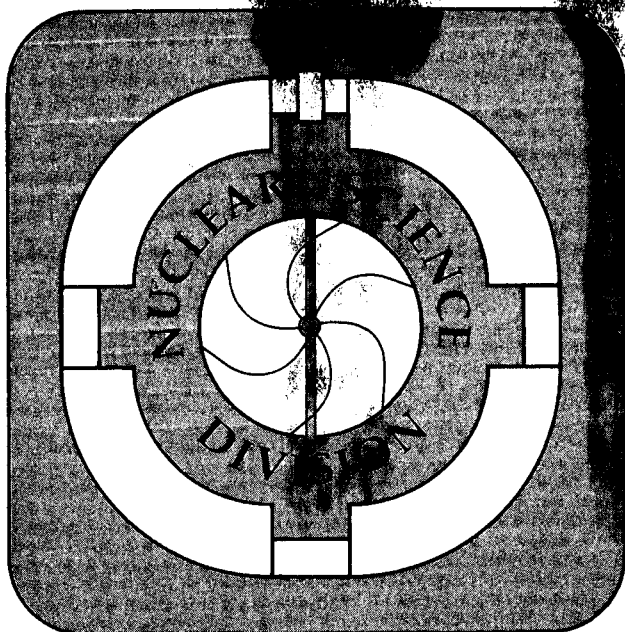
LIBRARY AND
DOCUMENTS SECTION

Submitted to Physics Letters B

TRANSPORT PROPERTIES OF EXCITED NUCLEAR MATTER
AND THE SHOCK-WAVE PROFILE

P. Danielewicz

May 1984



LBL-17707
c.2

DISCLAIMER

This document was prepared as an account of work sponsored by the United States Government. While this document is believed to contain correct information, neither the United States Government nor any agency thereof, nor the Regents of the University of California, nor any of their employees, makes any warranty, express or implied, or assumes any legal responsibility for the accuracy, completeness, or usefulness of any information, apparatus, product, or process disclosed, or represents that its use would not infringe privately owned rights. Reference herein to any specific commercial product, process, or service by its trade name, trademark, manufacturer, or otherwise, does not necessarily constitute or imply its endorsement, recommendation, or favoring by the United States Government or any agency thereof, or the Regents of the University of California. The views and opinions of authors expressed herein do not necessarily state or reflect those of the United States Government or any agency thereof or the Regents of the University of California.

Transport Properties of Excited Nuclear Matter and the Shock-Wave Profile*

P. Danielewicz[†]

Nuclear Science Division
Lawrence Berkeley Laboratory
University of California
Berkeley, California 94720

*This work was supported by the Director, Office of Energy Research, Division of Nuclear Physics of the Office of High Energy and Nuclear Physics of the U.S. Department of Energy under Contract DE-AC03-76SF00098.

[†]On leave of absence from the Institute of Theoretical Physics, Warsaw University, Warsaw, Poland

Transport Properties of Excited Nuclear Matter and the Shock-Wave Profile*

P. Danielewicz[†]

Nuclear Science Division
Lawrence Berkeley Laboratory
University of California
Berkeley, California 94720

Abstract

Shear viscosity and heat conduction coefficients of nuclear matter are derived from the Uhlenbeck-Uehling equation. The calculated coefficients exceed by a factor of two or more those used until now in hydrodynamic calculations of nuclear collisions. When applied to study a shock profile in nuclear matter, the coefficients yield results that are roughly consistent with cascade calculations. The study reveals that shock phenomena are not possible at energies $E_{\text{lab}} \lesssim 100$ MeV/nucleon, while at higher energies a fully developed shock wave requires heavy nuclei ($A \gtrsim 100$).

*This work was supported by the Director, Office of Energy Research, Division of Nuclear Physics of the Office of High Energy and Nuclear Physics of the U.S. Department of Energy under Contract DE-AC03-76SF00098.

[†]On leave of absence from the Institute of Theoretical Physics, Warsaw University, Warsaw, Poland

The hydrodynamic approach for intermediate-energy heavy-ion collisions has already undergone years of development. Surprisingly, however, one finds that a major ingredient of the approach, the magnitude of the transport coefficients, has not been settled and that the common microscopic results have not been explored. This is unfortunate since the high-temperature (low-density) microscopic results for the coefficients can be found in textbooks, e.g. [1]. Furthermore, the results for nuclear matter have been given in the literature even with the inclusion of relativistic kinematics [2]. The low-temperature behavior of the coefficients is also known, and for nuclear matter it has been studied first by Tomonaga [3]. In this paper we derive the expressions for the shear viscosity and heat conduction coefficients associated with the Uhlenbeck-Uehling equation. These extend the known results, smoothly interpolating between the known limits. Subsequently we examine the effect of the transport coefficients on the shock-wave profile in the collisions, with this being a second major topic of the paper. The results for the coefficients are subject to changes due to effects that go beyond the dynamics of the Uhlenbeck-Uehling equation and that are discussed at the end of the paper, but we believe that the equation, as it stands, is of sufficient conceptual significance for the heavy-ion collisions, to make it instructive and important to realize the results and implications.

The shear viscosity and heat conduction coefficients, η and κ , respectively, are the coefficients in the expansion of the hydrodynamic momentum T^{ij} and energy T^{0i} fluxes in the particle rest frame in terms of the macroscopic gradients:

$$T^{(1)ij} = -\eta \left(\frac{\partial v^i}{\partial x^j} + \frac{\partial v^j}{\partial x^i} - \frac{2}{3} \delta^{ij} \frac{\partial v^l}{\partial x^l} \right) \equiv -\eta v'^{ij} \quad , \quad (1)$$

$$\tau^{(1)0i} = -\kappa \frac{\partial T}{\partial x^i}, \quad (2)$$

where v is the fluid velocity, T is the temperature, and (2) is valid in the nonrelativistic limit. The elementary mean-free-path arguments yield:

$n \sim \frac{1}{3} n m u \lambda$ and $\kappa \sim \frac{1}{3} n c u \lambda$, with the particle density n , mass m , average velocity u , mean free path λ , and the specific heat per particle c . In order to fix the attention let us see what these estimates imply for the nuclear medium. With $\lambda \approx (n\sigma)^{-1}$, where σ is the particle-particle cross-section, and the Boltzmann statistics limit $c = \frac{3}{2}$, one finds $n \sim \frac{1}{3} \frac{m u}{\sigma} \approx \frac{1}{\sigma} \left(\frac{mT}{3}\right)^{1/2}$ and $\kappa \sim \frac{1}{2\sigma} \left(\frac{3T}{m}\right)^{1/2}$,

independent of density. Taking for the N-N cross-section $\sigma \approx 40$ mb, we get $n \sim 4.4 (T/\text{MeV})^{1/2} \text{ MeV}/\text{fm}^2 c$ and $\kappa \sim 0.007 (T/\text{MeV})^{1/2} c/\text{fm}^2$. For the temperature $T \sim 60$ MeV, the mean-free-path estimate yields $n \sim 34 \text{ MeV}/\text{fm}^2 c$ and $\kappa \sim 0.055 c/\text{fm}^2$,

which may be compared with the values used in the hydrodynamic calculations:

$n = 6 \text{ MeV}/\text{fm}^2 c$ [4], $n = (5 - 25) \text{ MeV}/\text{fm}^2 c$ (when $T < 100$ MeV) [5,6], and $\kappa = 0.015 c/\text{fm}^3$ [6] (cf. also Refs. [7]).

At low temperatures the mean free path in the fermion system diverges as $\lambda \propto T^{-2}$, and the coefficients diverge as $n \propto T^{-2}$ and $\kappa \propto T^{-1}$, respectively. We get the more fundamental results for the coefficients by solving the Uhlenbeck-Uehling equation linearized in the gradients

$$D_a f_a^0 = \frac{g}{(2\pi)^3} \int d^3 p_b \int d\Omega' \frac{d\sigma}{d\Omega'} \frac{|p_a - p_b|}{m} f_a^0 f_b^0 \tilde{f}_a^0 \tilde{f}_b^0 \times (\chi_{a'} + \chi_{b'} - \chi_a - \chi_b), \quad (3)$$

for the deviation δf of the distribution function $f(p, x, t)$ from equilibrium f^0 , $\delta f = \chi f^0 \tilde{f}^0$, with $\tilde{f} = 1 - f$, and here $D \equiv \left(\frac{\partial}{\partial t} + \frac{p}{m} \cdot \frac{\partial}{\partial x}\right)$. The system is taken to be spin-isospin symmetric, with the degeneracy factor $g = 4$ (it drops though from the transport coefficients). The differential cross-section $d\sigma/d\Omega'$ in (3) is spin-isospin averaged, and consequently the integration $d\Omega'$

runs only over half of the solid angle. Assuming $\text{div } \underline{v} = 0$ ($\text{div } \underline{v}$ drives the bulk viscosity which may be considered negligible here [2,8]), $Df^0 = \frac{1}{2mT} f^0 f^0 [(p^i p^j - \frac{1}{3} \delta^{ij} p^2) v'^{ij} + \frac{1}{mT} (p^2 - \frac{5}{3} \langle p^2 \rangle) p^i \frac{\partial T}{\partial x^i}]$, with the average $\langle p^2 \rangle$ taken over the distribution. We search for χ of the form $\chi = c_1 (p^i p^j - \frac{1}{3} \delta^{ij} p^2) v'^{ij} + c_2 (p^2 - \frac{5}{3} \langle p^2 \rangle) p^i \frac{\partial T}{\partial x^i}$, and we fix the constants in the expression by multiplying both sides of (3) by χ_a and integrating over the momenta. Upon evaluating the fluxes from δf we find:

$$n' = \frac{5}{9} mT \left(\int_0^\infty dp p^4 f^0 \right)^2 / \int_0^\infty dp_a p_a^2 \int_0^\infty dp_b p_b^2 \int d\cos\theta_{ab} \int d\Omega' \times \frac{d\sigma}{d\Omega'} \sin^2 \theta' f_a^0 f_b^0 \tilde{f}_a^0 \tilde{f}_b^0 q_{ab}^5, \quad (4)$$

$$\kappa = \frac{1}{27m} \left(21 \int_0^\infty dp p^6 f^0 - 25 \left(\int_0^\infty dp p^4 f^0 \right)^2 / \int_0^\infty dp p^2 f^0 \right)^2 / \int_0^\infty dp_a p_a^2 \int_0^\infty dp_b p_b^2 \int d\cos\theta_{ab} \int d\Omega' \frac{d\sigma}{d\Omega'} f_a^0 f_b^0 \tilde{f}_a^0 \tilde{f}_b^0 \times q_{ab}^3 [(p_b^2 - p_a^2)^2 + (p_b^2 - p_a^2)^2 - 2(p_b^2 - p_a^2)(p_b^2 - p_a^2) \cos \theta'] \quad (5)$$

with $q_{ab} = \frac{1}{2} |p_a - p_b|$. The results from (4) and (5), using the polynomial fits [9] to the experimental N-N cross-sections, are displayed in Fig. 1. By the variational principle [10] for the transport coefficients, Eqs. (4) and (5) are only lower bounds for the coefficients associated with the kinetic equation. The well explored limits can be examined though. In the Boltzmann statistics limit we obtain, from (4) and (5),

$$n = \frac{5\sqrt{\pi}}{16} \frac{\sqrt{mT}}{\tilde{\sigma}} \quad , \quad \kappa = \frac{75\sqrt{\pi}}{64} \frac{1}{\tilde{\sigma}} \sqrt{\frac{T}{m}} \quad , \quad (6)$$

with

$$\tilde{\sigma} = \frac{1}{4} \int_0^\infty d\left(\frac{q^2}{mT}\right) \left(\frac{q^2}{mT}\right)^3 e^{-\frac{q^2}{mT}} \int d\cos\theta' \frac{d\sigma}{d\cos\theta'} \sin^2\theta' . \quad (7)$$

These results are the first-order Chapman-Enskog coefficients [11,1]. The higher-order corrections typically raise η by only 1.5% and κ by 2.5%. The low-temperature expansion of (4) and (5) leads to

$$\eta = \frac{1}{16\pi^2} \frac{p_F^5}{m^2 \tilde{\sigma}_1} \frac{1}{T^2} , \quad \kappa = \frac{5}{96} \frac{p_F^3}{m^2 \tilde{\sigma}_2} \frac{1}{T} , \quad (8)$$

where p_F is the Fermi momentum, and

$$\begin{aligned} \tilde{\sigma}_1 &= \frac{15}{16\pi} \int d\theta_{ab} \sin^5 \frac{\theta_{ab}}{2} \int d\theta' \frac{d\sigma}{d\cos\theta'} \sin^2\theta' , \\ \tilde{\sigma}_2 &= \frac{3}{4\pi} \int d\theta_{ab} \sin^3 \frac{\theta_{ab}}{2} \int d\theta' \frac{d\sigma}{d\cos\theta'} . \end{aligned} \quad (9)$$

The exact low-temperature solution [8] to the Uhlenbeck-Uehling equation with the experimental cross-sections leads to η larger by ~2% and κ by ~12% for densities $(1-4)n_0$ (Eqs. (8) correspond to $c(\lambda_{2s}) = \frac{3}{4}$ and $H(\lambda_{1a}) = \frac{5}{12}$ of Ref. [8]). Eqs. (7) and (9) are normalized so that for an isotropic energy-independent cross-section $\tilde{\sigma} \equiv \tilde{\sigma}$, and $\tilde{\sigma}_1 \equiv \tilde{\sigma}_2 = \sigma$. (For the scrupulous reader let us mention in connection with (9) that the low-temperature expansion and the limit of a forward peaked cross-section are not interchangeable.) In both (7) and (9), and already in (4) and (5), it can be seen that high momenta are most effective in transport in the medium. The q^2/mT weight in (7) is maximized in particular at a two-particle $E_{lab} = 2q^2/m = 6T$. For temperatures $T \gtrsim 80$ MeV one cannot ignore the fact that a finite portion of the N-N cross-section is inelastic. In calculating the results of Fig. 1 we add the inelastic cross-section as an isotropic contribution to the elastic cross-section, and this has, in fact, some justification close to the inelastic threshold.

For reference we list analytic fits to the results from (4) and (5):

$$n = \frac{1700}{T^2} \left(\frac{n}{n_0} \right)^2 + \frac{22}{1 + T^2 \cdot 10^{-3}} \left(\frac{n}{n_0} \right)^{0.7} + \frac{5.8T^{1/2}}{1 + 160/T^2} , \quad (10)$$

$$\kappa = \frac{0.15}{T} \left(\frac{n}{n_0} \right)^{1.4} + \frac{0.02}{1 + T^4/7 \cdot 10^6} \left(\frac{n}{n_0} \right)^{0.4} + \frac{0.0225T^{1/2}}{1 + 160/T^2} , \quad (11)$$

where n is in $\text{MeV}/\text{fm}^2 c$, κ in c/fm^2 , T in MeV, and $n_0 = 0.145 \text{ fm}^{-3}$. The middle terms merely serve the purpose of the fit. Also for reference we list rough fits to the relaxation times that follow from relating the transport coefficients to the relaxation time equation [12]:

$$\tau_n \frac{n}{n_0} \approx \frac{850}{T^2} \left(\frac{n}{n_0} \right)^{4/3} \left(1 + 0.04T \left(\frac{n_0}{n} \right) \right) + \frac{38T^{-1/2}}{1 + 160/T^2} , \quad (12)$$

$$\tau_\kappa \frac{n}{n_0} \approx \frac{310}{T^2} \left(\frac{n}{n_0} \right)^{1.4} \left(1 + 0.1T \left(\frac{n_0}{n} \right) \right) + \frac{57T^{-1/2}}{1 + 160/T^2} , \quad (13)$$

with τ in fm/c . Clearly, the system exhibits different relaxation times under different symmetries of the disturbance. With nuclear sizes taken into account, it follows from (12) and (13) that for the temperatures $T \lesssim 6$ MeV in moderate size nuclei, the one-body dissipation (interactions with the nuclear surface) starts to dominate over the effects associated with the two-body interactions.

We now demonstrate the importance of the transport coefficients by solving the relativistic hydrodynamic equations with dissipative terms (the relativistic Navier-Stokes equations) for the shock profile in nuclear matter corresponding to a projectile bombarding energy in the range $E_{\text{lab}} \leq 800 \text{ MeV}/\text{nucl}$. We use a typical equation of state [13,14] consisting of kinetic and potential parts. In the compressional part of the energy per nucleon $W_c = K(n - n_0)^2/18nn_0$, the compressibility K is set equal to 210 MeV. The properties of the matter in the two regions away from the shock front are related by the Rankine-

Hugoniot equation, and an extra constraint on the parameters of the heated matter is provided by the bombarding energy per nucleon [13]. In the shock frame the flow of matter is stationary, and one can exploit the conservation of the hydrodynamic fluxes to obtain the following equations (in the Eckart choice of the hydrodynamic rest-frame [15]):

$$nu^z = (nu^z)_0, \quad (14)$$

$$\frac{du^z}{dz} = \frac{3}{4} \frac{P(u^0)^2 - e(u^z)^2 - (\tau^{zz})_0((u^0)^2 + (u^z)^2) + 2(\tau^{0z})_0 u^0 u^z}{n(u^0)^2}, \quad (15)$$

$$\frac{d}{dz} \frac{\mu}{T} = \frac{e + P}{nT^2} \frac{-eu^z + (\tau^{0z})_0 u^0 - (\tau^{zz})_0 u^z}{(u^0)^2}, \quad (16)$$

with the four-velocity $u \equiv (\gamma, \gamma \underline{v})$, energy density e , pressure P , the direction of the shock wave propagation z , chemical potential μ , and $(\cdot)_0$ referring to fluxes in the asymptotic regions away from the shock front. Eq. (16) reflects the fact that relativistically the heat conduction is driven by μ/T [15,16]. Nonrelativistically μ reduces to m , and T becomes the driving force (2). To avoid difficulties with handling the zero-temperature divergences, the temperature of the intact matter is set equal to 1 MeV. In order to start Eqs. (14-16), the state of matter has to be slightly different from any of the asymptotic regions. Assuming a variation of u^z , the variation of μ/T can be found from de l'Hôpital's rule. Setting the heat conductivity $\kappa = 0$ in a calculation corresponds to keeping the numerator of the right hand side of Eq. (16) equal to zero throughout the shock wave, in an analogy with Eq. (14). The solutions to Eqs. (14-16) (or the nonrelativistic reduction of the set) are easy to generate, and in general might be used for testing hydrodynamic codes devised for handling more complicated problems. In Fig. 2 we present the rest-frame density, temperature, and pressure profiles of a shock wave

corresponding to $E_{lab} = 400$ MeV/nucleon. The profiles A and B are calculated using the present results for transport coefficients, and for illustration we include the profiles calculated using previous viscosity coefficients: profiles C with the largest of the coefficients in Ref. [6] $\eta = 18.6 (1 + T/120 \text{ MeV})^{1/2} \text{ MeV/fm}^2 c$, and profiles D with $\eta = 6 \text{ MeV/fm}^2 c$ of Refs. [4]. For the curves B, C, and D, the heat conductivity $\kappa = 0$. The transport coefficients introduce a scale having the dimension of a length into the hydrodynamic equations $\eta v/P \sim \lambda$, and the profiles B, C, and D exhibit a scaling which may be directly read off from Eq. (15). Namely, in the calculation based on Ref. [6], the average viscosity in the shock front is $\eta \approx 21 \text{ MeV/fm}^2 c$, and the profiles C are by a factor of about 3.5 extended along the z axis in comparison with the profiles D, where $\eta = 6 \text{ MeV/fm}^2 c$. For the curves B the average viscosity is $\eta \sim 60 \text{ MeV/fm}^2 c$, cf. Fig. 1, and the profiles are about 10 times broader than the profiles D! Upon switching on the heat conductivity (curves A in Fig. 2), the most amazing result is the slow fall-off of the temperature. Note, however, that it is relatively easy to raise the temperature in the degenerate Fermi gas without raising either the pressure or the energy density much. In fact, the pressure profile A in Fig. 2 follows approximately the shape of the density profile A. Variation of the density profiles with the bombarding energy is shown in Fig. 3a. The profiles are calculated with the present transport coefficients, and the 400 MeV/nucleon profile is here identical with the profile A of Fig. 2. The 70% of the Rankine-Hugoniot (asymptotic) density rise in Fig. 3a is found to occur at distances of 4.5, 2.9, 2.1, and 1.8 fm, for $E_{lab} = 100, 200, 400,$ and 800 MeV/nucleon, respectively. The above shock-frame distances contain amounts of matter equivalent respectively to distances in normal nuclear matter of 8., 5.7, 4.7, and 4.4 fm. The shock widths conventionally defined by the 70%

density rise, are shown in Fig. 3b in terms of the bombarding energy. Additionally, Fig. 3b displays the shock widths extracted from the cascade calculations [17,18]. Since the underlying dynamic assumptions are similar, the observed rough agreement is not a surprise. To the extent of their overlap, the current hydrodynamic results further seem to agree with the findings of a shock wave study using a simplified kinetic approach [19]. Let us now discuss the rapid rise of the shock widths with decreasing energy per nucleon in Fig. 3b. The point is that, irrespective of the zero-temperature divergence of the transport coefficients, the width of a shock wave is known to increase to infinity as the shock strength decreases (Mach number tends to unity), see e.g. [16]. The divergence of the coefficients implies only a stronger divergence [20] of a shock width as compared with that in classical gases [16]. It follows from Fig. 3b that shock phenomena are not possible in nuclear collisions at energies $E_{lab} \leq 100$ MeV/nuc1. At higher energies, the full shock development with the associated creation of high-density equilibrated matter would require rather heavy ($A \geq 100$) nuclei. In the view of the above, it would clearly be useful to learn the effect of the proper magnitudes of the transport coefficients in the calculations taking full account of the nuclear collision geometry [21,6,7]. On general grounds, one can expect the coefficients to bring the hydrodynamics closer to the cascade type of dynamics.*

Before concluding, we would like to discuss the possible modifications to the results for the coefficients. These seem to point towards even higher

*We should further comment here on the shock profiles from Ne + U collisions presented in Fig. 3 of Ref. [6]. Due to a combination of the large impact parameter, surface diffuseness, and small projectile size, the developing shock wave is fairly weak. It follows from the density that the shock corresponds to about 50 MeV/nuc1 in Fig. 3b. This explains the relatively large extension of profiles in [6] despite the small values of viscosity.

values of the coefficients than calculated here. First of all, under an assumption that the effective mass expansion holds for the relevant part of the 1-particle spectrum, $\epsilon(\underline{p}, \underline{r}, t) \approx p^2/2m^*(\underline{r}, t) + \epsilon_0(\underline{r}, t)$, the results (4-9) can be rederived starting from the Landau rather than Uhlenbeck-Uehling equation. All the explicit masses m in (4-8) are formally replaced by m^* , and at low temperatures a strong effective-mass dependence is observed (8), which weakens at high temperatures (6). With the current [22] $m^*/m = (0.8-1)$, an effective mass $m^* \sim 0.8$ would enhance by 50% the low-temperature coefficients. Furthermore, the medium is likely to cut down the values of the cross-sections, though presumably least for high relative momenta. With (10) and (11), the $n = n_0$ cross-sections at low temperatures, (8) and (9), are $\tilde{\sigma}_1 \approx 45$ mb and $\tilde{\sigma}_2 \approx 65$ mb, and consequently κ is more likely to change than η . Enhancement of the low-temperature coefficients would tend to push the low-energy rise in Fig. 3b towards higher energies. At high temperatures and densities, the effects of the finite size of the 2-particle interaction zone, and, in particular, the so-called collisional transfer (mediation of the momentum and energy by the potential), may become important, as pointed out by Malfliet [23]. The only rigorously developed method that addresses the problem, and is capable of providing simple expressions for the coefficients, is the Enskog theory of the hard sphere gas [24,11]. Because of its simplicity, the theory is frequently used in describing real classical gases [25]. The theory looks for corrections to the Chapman-Enskog transport coefficients, in terms of powers of nb , where $b = \frac{2\pi}{3} d^3$ and d is the hard sphere diameter. If one proceeded as for classical gases, then the hard sphere diameter should be identified at low densities from the effective cross-section $d = (\tilde{\sigma}/\pi)^{1/2} \approx 1.0$ fm. The Enskog theory would then imply a $\sim 15\%$ rise over the Chapman-Enskog coefficients at the normal nuclear density, and a factor of 2 enhancement of the coefficients at

$n \sim 3n_0$, due to collisional transfer. While the rise of the nuclear-matter coefficients with density on account of the collisional transfer is plausible, the rise need not be as rapid. Namely much of the rise of coefficients in the Enskog method stems from the fact that the momentum and energy, otherwise transported through the medium with the particle velocities, get instantaneously transported over the diameter of the sphere when the particles enter the interaction range. While this is seemingly a good approximation for classical gases, it is certainly not the case for the problem at hand, even by the mere consideration of relativity. (The latter point might be best illustrated by an observation that at temperature $T \sim 80$ MeV, the speed of sound of an excluded volume gas, $c_s = \frac{1}{1 - nb} \sqrt{\frac{5T}{3m}}$, violates the light velocity at just about the same density for which the Enskog corrections to the coefficients become sizable.) In any case, if there were a significant enhancement of the coefficients with density, it would act to bend the curves of Fig. 3b upwards for the higher energies in the figure. When the inelastic processes become important, the kinetic results for the coefficients could be improved by writing down a set of kinetic equations and solving them for the coefficients, possibly in a similar manner as in this paper. Delays associated with the production and absorption of particles might bring about a finite value of bulk viscosity [16,26] (just as might the collisional transfer, as indicated by the Enskog theory). With a rise in temperature, the number of particles could soon become too cumbersome to handle, and moreover, the physics too uncertain, that one might be forced to use the simplest estimates [27]. Ultimately, the transport coefficients of the nuclear medium should be sought after using the many-body methods from the Kubo formulae [28]. This task is definitely not trivial if one aims at more than just recovering the results which could be obtained from a kinetic equation [29,30]. Before this can be accomplished we

hope that the current results for the coefficients can serve as a useful reference.

Acknowledgements

Discussions with M. Gyulassy have substantially contributed to the content of the paper. The author acknowledges also comments from H. S. Köhler.

This work was supported by the Director, Office of Energy Research, Division of Nuclear Physics of the Office of High Energy and Nuclear Physics of the U.S. Department of Energy under Contract DE-AC03-76SF00098.

References

- [1] E. H. Kennard, Kinetic Theory of Gases (McGraw-Hill, New York, 1938);
F. Reif, Fundamentals of Statistical and Thermal Physics (McGraw-Hill, New York, 1965).
- [2] V. M. Galitskii, Yu. B. Ivanov, and V. A. Khangulyan, Yad. Fiz. 30 (1979) 778 [Sov. J. Nucl. Phys. 30 (1979) 401].
- [3] S. Tomonaga, Z. Phys. 110 (1938) 573.
- [4] L. P. Csernai, B. Lukács, and J. Zimányi, Proc. Int. Workshop on Gross Properties of Nuclei and Nuclear Excitations VII, Hirschegg, 1979, ed. H. Feldmeier (Technische Hochschule Darmstadt, 1979), p. 133; Lett. Nuovo Cimento 27 (1980) 111;
L. P. Csernai, H. W. Barz, B. Lukács, and J. Zimányi, Proc. EPS Topical Conf. on Large Amplitude Collective Nuclear Motions, Keszthely, 1979 (Central Research Institute for Physics, Budapest, 1979), p. 533;
L. P. Csernai and B. Lukács, Viscous Hydrodynamical Model for Relativistic Heavy-Ion Collisions, Central Research Institute for Physics Report KFKI-1979-58 (1979); Acta Phys. Pol. B15 (1984) 149.

- [5] L. P. Csernai and H. W. Barz, Z. Phys. 296 (1980) 173.
- [6] G. Buchwald, L. P. Csernai, J. A. Maruhn, W. Greiner, and H. Stöcker, Phys. Rev. C24 (1981) 135.
- [7] H. H. K. Tang and C. Y. Wong, Phys. Rev. C21 (1980) 1846; C26 (1982) 284; L. P. Csernai and H. Stöcker, *ibid.* C25 (1982) 3208.
- [8] J. Sykes and G. A. Brooker, Ann. Phys. (N.Y.) 56 (1970) 1.
- [9] T. P. Clements and L. Winsberg, Polynomial Fits of Nucleon-Nucleon Scattering Data, Lawrence Radiation Laboratory Report UCRL-9043 (1960).
- [10] E. J. Hellund and E. A. Uehling, Phys. Rev. 56 (1939) 818.
- [11] S. Chapman and T. G. Cowling, The Mathematical Theory of Non-uniform Gases (Cambridge University Press, New York, 1960).
- [12] H. S. Köhler, Nucl. Phys. A378 (1982) 159.
- [13] H. G. Baumgardt, J. U. Schott, Y. Sakamoto, E. Schopper, H. Stöcker, J. Hofmann, W. Scheid, and W. Greiner, Z. Phys. A273 (1975) 359.
- [14] P. Danielewicz, Nucl. Phys. A314 (1979) 465.
- [15] S. R. de Groot, W. A. van Leeuwen, and Ch. G. van Weert, Relativistic Kinetic Theory (North-Holland, Amsterdam, 1980).
- [16] L. D. Landau and E. M. Lifschitz, Fluid Mechanics (Pergamon Press, Oxford, 1982).
- [17] E. C. Halbert, Phys. Rev. C28 (1981) 295.
- [18] J. Cugnon, T. Mizutani, and J. Vandermeulen, Nucl. Phys. A352 (1981) 505.
- [19] J. Bondorf, Yu. B. Ivanov, and J. Zimányi, Physica Scripta 24 (1981) 514.
- [20] V. M. Galitskii, Pis'ma v Zh. Eksp. Teor. Fiz. 25 (1977) 175 [JETP Lett. 25 (1977) 160].
- [21] G. Buchwald, G. Graebner, J. Theis, J. A. Maruhn, W. Greiner, and H. Stöcker, Phys. Rev. C28 (1983) 1119; L. Csernai, H. Stöcker, P. R. Subramanian, G. Buchwald, G. Graebner, A. Rosenhauer, J. A. Maruhn, and W. Greiner, *ibid.* C28 (1983) 2001.

- [22] M. R. Anastasio, L. S. Celenza, W. S. Pong, and C. M. Shakin, Phys. Reports 100 (1983) 327.
- [23] R. Malfliet, Transport Properties of Nuclear Matter at High Densities and High Temperatures, Kernfysisch Versneller Instituut Report KVI-458 (1983).
- [24] D. Enskog, Kungliga Svenska Vetenskapsakademiens Handlingar Ny Föld 63 (4) (1922) [in: Kinetic Theory, vol. 3, ed. S. G. Brush (Pergamon Press, Oxford, 1972), p. 226].
- [25] M. G. Velarde, in: Transport Phenomena, Ed. G. Kirczenow and J. Maro (Lecture Notes in Physics, vol. 31, Springer, Berlin, 1974), p. 288.
- [26] A. Hosoya and K. Kajantie, Transport Coefficients of QCD Matter, Helsinki University Report HU-TFT-83-62 (1983).
- [27] P. Danielewicz and M. Gyulassy, Dissipative Phenomena in Quark Gluon Plasmas, Lawrence Berkeley Laboratory Report LBL-17278 (1984).
- [28] R. Kubo, J. Phys. Soc. Japan 12 (1957) 570.
- [29] A. Hosoya, M. Sakagami, and M. Takao, Nonequilibrium Thermodynamics in Field Theory. Transport Coefficients, Osaka University Report OU-HET 53 (1983), Ann. Phys. (N.Y.) in press.
- [30] P. Danielewicz, Ann. Phys. (N.Y.) 152 (1984) 239, 305.

Figure Captions

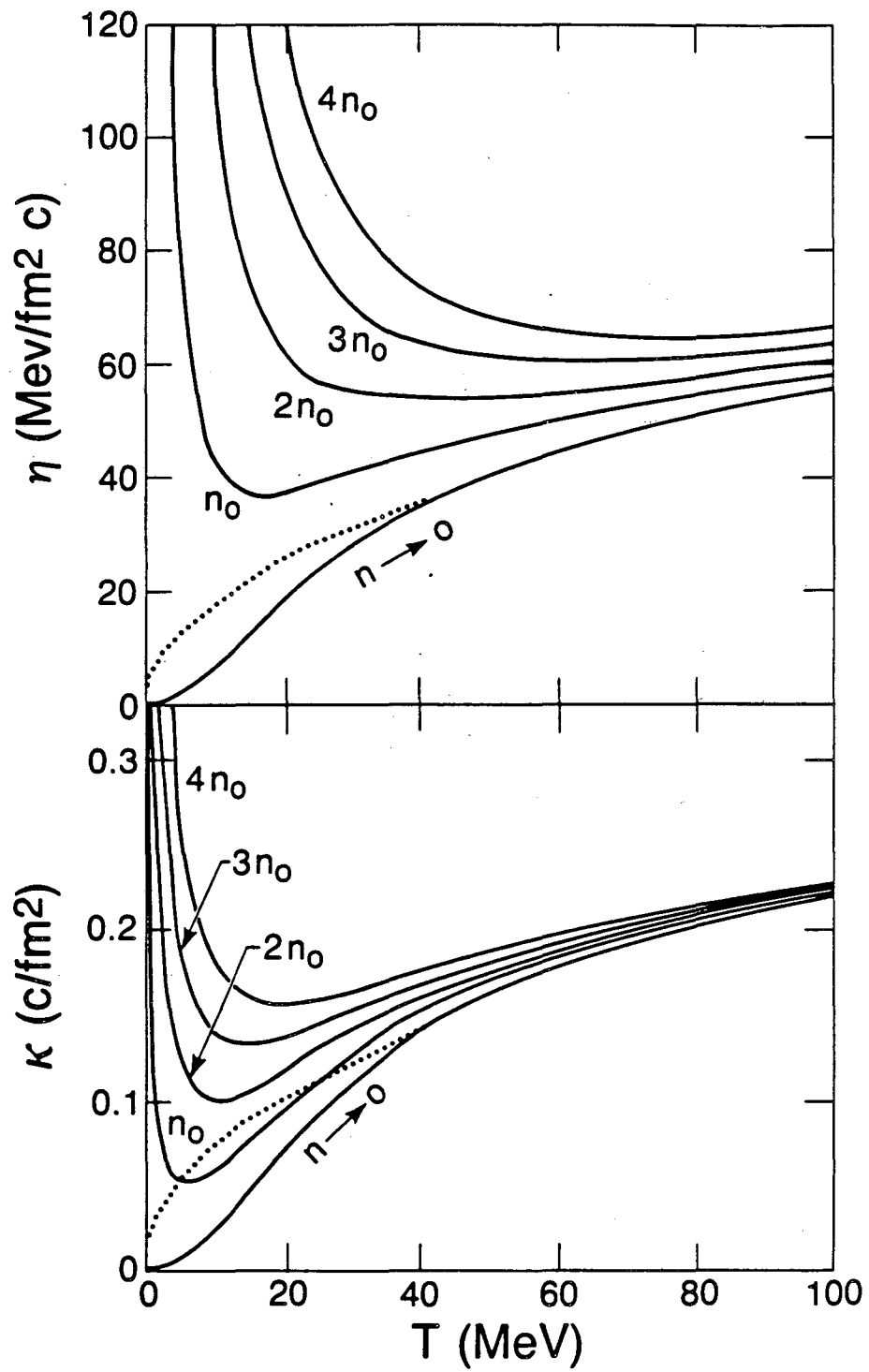
- Fig. 1 The temperature and density dependence of the nuclear-matter transport coefficients. The normal nuclear density has been taken as $n_0 = 0.145 \text{ fm}^{-3}$. Dotted lines denote the Chapman-Enskog results (6), with the effective cross-section set equal to $\tilde{\sigma} = 30 \text{ mb}$.
- Fig. 2 Rest-frame density n , temperature T , and pressure P , as functions of the distance z in the shock-wave frame. The shock wave corresponds

here to $E_{lab} = 400$ MeV/nuc1. Curves A and B are calculated using the transport coefficients from Fig. 1, curves C with $n = 18.6 (1 + T/120 \text{ MeV})^{1/2} \text{ MeV/fm}^2 c$ of Ref. [6], and curves D with $n = 6 \text{ MeV/fm}^2 c$ of Refs. [4]. For the curves B, C, and D, $\kappa = 0$. The origin of the z axis is arbitrary, but it is identical throughout the figure for each of the sets (A, B, C, or D).

Fig. 3 (a) Rest-frame nuclear-matter densities as functions of the distance z in the shock-wave frame. Numbers in the figure designate the projectile bombarding-energy in MeV/nuc1 to which the shock corresponds.

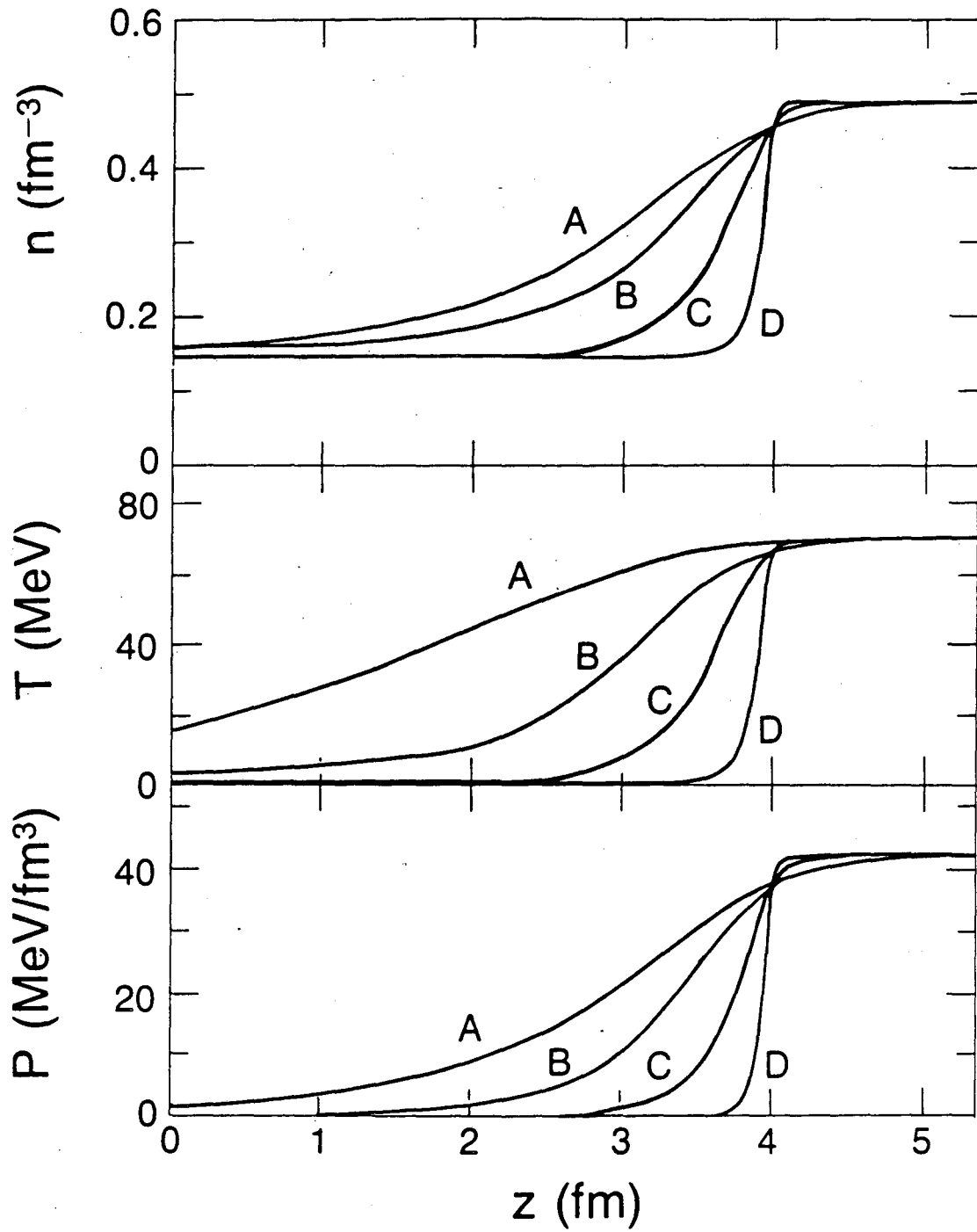
(b) Bombarding-energy variation of the shock widths which are defined by the 70% of the asymptotic density rise. The upper curve is in terms of the distance in normal nuclear-matter (see text). Continuation with the dashed lines emphasizes the increasing abundance of π mesons and Δ resonances that are not included in the treatment. The dashed areas and the error bar represent the shock widths extracted from cascade calculations [17,18]. Note that in the Halbert [17] cascade, the nucleons are at rest on the intact matter side (Boltzmann statistics with $T = 0$) and the cross sections are energy independent; consequently, the shock-wave density profiles do not depend on energy. This is (up to relativity) preserved in the hydrodynamic formulation of the cascade dynamics, and we have used it as one of the tests for our calculations. (One is always in the Mach number $M \rightarrow \infty$ limit; the sound velocity ahead of the shock is 0.) In an attempt at a hydrodynamic formulation of the Cugnon [18] cascade type of dynamics, where nucleons are given Fermi momenta on the intact side, we took Boltzmann statistics with

$T = 23$ MeV for the intact side and $\tilde{\sigma} \equiv 30$ mb in (6). The widths increase at low bombarding energies, but not as quickly as in the regular hydrodynamic calculation. In both simulations of the cascade dynamics, the widths are slightly larger than the regular ones for higher bombarding energies.



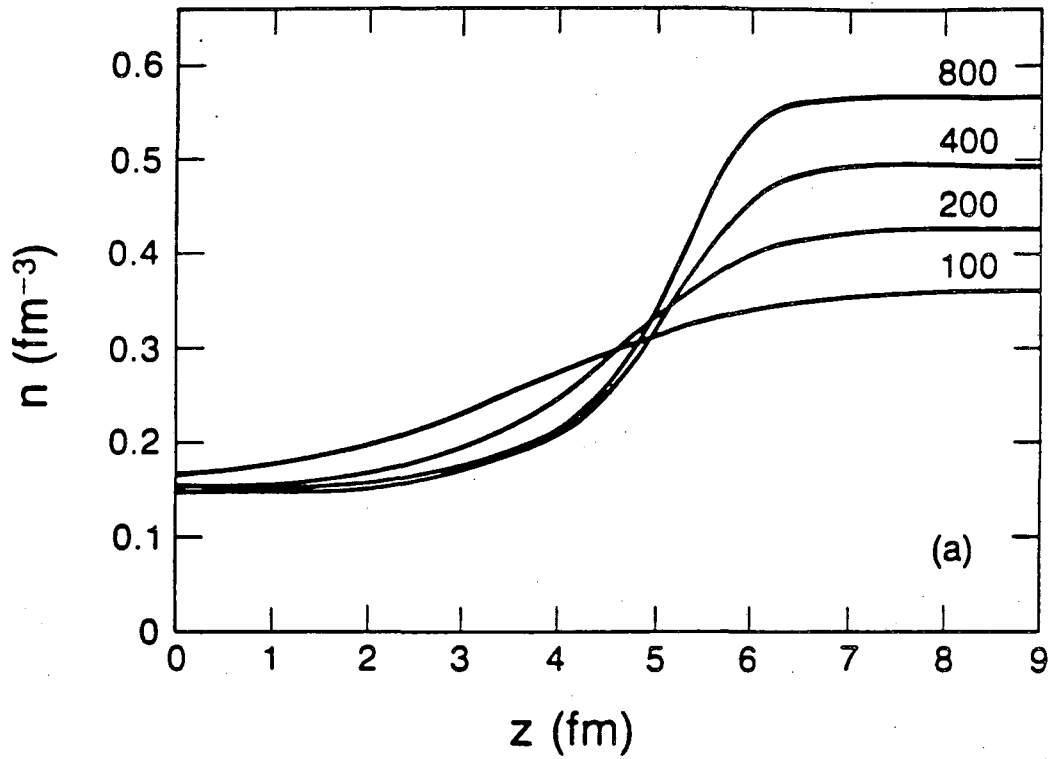
XBL 842-10062A

Fig. 1



XBL 842-10074

Fig. 2



XBL 842-10073

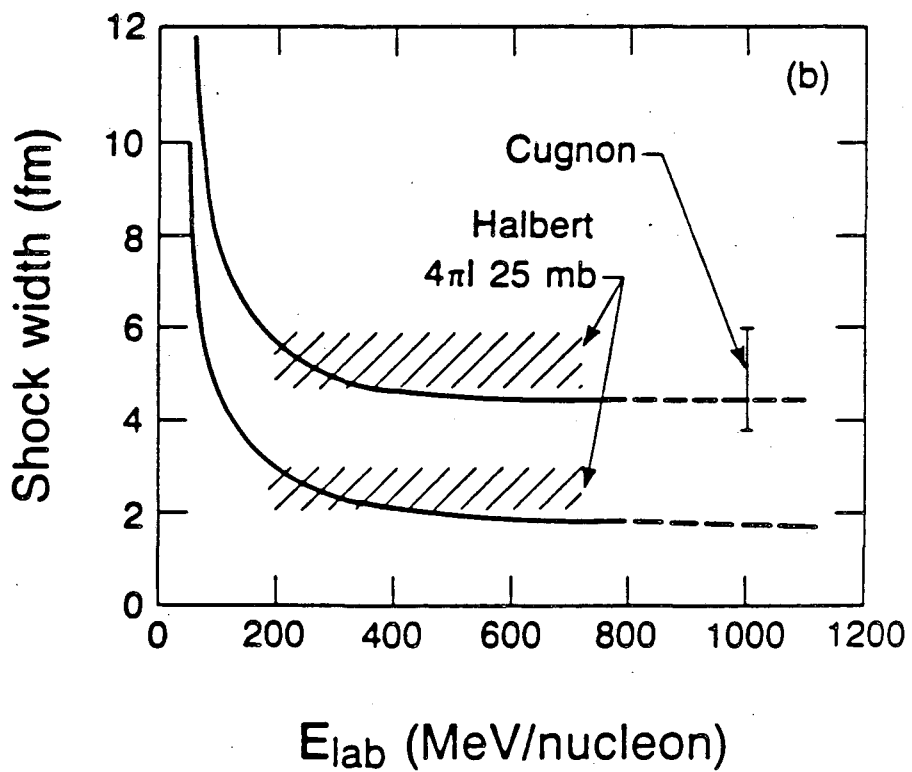


Fig. 3

XBL 844-10402

This report was done with support from the Department of Energy. Any conclusions or opinions expressed in this report represent solely those of the author(s) and not necessarily those of The Regents of the University of California, the Lawrence Berkeley Laboratory or the Department of Energy.

Reference to a company or product name does not imply approval or recommendation of the product by the University of California or the U.S. Department of Energy to the exclusion of others that may be suitable.

TECHNICAL INFORMATION DEPARTMENT
LAWRENCE BERKELEY LABORATORY
UNIVERSITY OF CALIFORNIA
BERKELEY, CALIFORNIA 94720